Natural Resources Canada   Ressources naturelles Canada

GEOMATICS CANADA
OPEN FILE 64

Emergency Geomatics Service activation for Turtle Mountain, Alberta InSAR monitoring

B. Lehrbass, S. Samsonov, J. Dudley, N. Svacina, H. Drouin, V. Decker, and S. Tolszczuk-Leclerc

2021

Canada

GEOMATICS CANADA
OPEN FILE 64

Emergency Geomatics Service activation for Turtle Mountain, Alberta InSAR monitoring

B. Lehrbass, S. Samsonov, J. Dudley, N. Svacina, H. Drouin,
V. Decker, and S. Tolszczuk-Leclerc

Canada Centre for Mapping and Earth Observation, 560 Rochester Street, Ottawa, Ontario

2021

Permanent link: https://doi.org/10.4095/328268

This publication is available for free download through GEOSCAN (https://geoscan.nrcan.gc.ca/).

Recommended citation
Lehrbass, B., Samsonov, S., Dudley, J., Svacina, N., Drouin, H., Decker, V., and Tolszczuk-Leclerc, S., 2021. Emergency Geomatics Service activation for Turtle Mountain, Alberta InSAR monitoring; Geomatics Canada, Open File 64, 19 p. https://doi.org/10.4095/328268

Publications in this series have not been edited; they are released as submitted by the author.

ABSTRACT

The Frank Slide in 1903 caused the deaths of more than 70 people, and there remains a risk of a second rock avalanche. Since then, many different methods have been used to monitor the slope for signs of movement. On April 8, 2020, the Alberta Energy Regulator (AER) contacted the Canada Centre for Mapping and Earth Observation (CCMEO) with a request for emergency assistance to monitor Turtle Mountain for deformation using interferometric synthetic aperture radar following the hardware failure of their ground-based monitoring system. This report describes at a high level the communication, planning, setup, operation, and reporting for this emergency request. Each deformation monitoring program presents a unique challenge, but this methodology can be broadly adapted to similar InSAR monitoring requests in the future. The purpose of this report is to provide a record of the services provided to help guide future geohazards monitoring requests, which may become more frequent with increased landslide risk due to climate change and greater satellite data availability.

Between April 8 and June 30, 2020, 40 images were collected by RADARSAT-2 and RADARSAT Constellation Mission satellites over Turtle Mountain. These images were processed quickly after acquisition and no significant deformation was observed during the monitoring period. Historical deformation of up to 5 cm in the line-of-sight was observed between 2014 and 2020.

Contents

PLAIN LANGUAGE SUMMARY

The Alberta Geological Survey (AGS), a branch of the Alberta Energy Regulator (AER), is responsible for the long-term monitoring of a potential landslide at Turtle Mountain. They provide a near real-time ground-based remote monitoring network as part of their Turtle Mountain Monitoring Program. Following the hardware failure of their ground-based InSAR monitoring system on April 8, 2020, the AER contacted the Canada Centre for Mapping and Earth Observation (CCMEO) with a request for emergency assistance to monitor Turtle Mountain for deformation using interferometric synthetic aperture radar (InSAR) with the RADARSAT Constellation Mission and RADARSAT-2. Emergency management and contingency plans were then activated until June 10, 2020, when the AER confirmed that the ground-based InSAR system had been repaired and was collecting valid data. This report summarizes the project setup and monitoring that was performed during the EGS activation.

RÉSUMÉ EN LANGAGE CLAIR

L'Alberta Geological Survey (AGS), une branche de l'Alberta Energy Regulator (AER), est responsable de la surveillance à long terme d'un glissement de terrain potentiel à Turtle Mountain. Ils opèrent un réseau de surveillance au sol en temps quasi réel dans le cadre de leur programme de surveillance de Turtle Mountain. Suite à la défaillance matérielle de leur système de surveillance au sol le 8 avril 2020, l'AER a contacté le Centre canadien de cartographie et d'observation de la Terre (CCCOT) avec une demande d'aide d'urgence pour surveiller la déformation de Turtle Mountain par interférométrie satellitaire à l'aide d'un radar à synthèse d'ouverture (InSAR) avec la mission de la Constellation RADARSAT (MCR) et RADARSAT-2. Les plans de mesures d'urgence et de contingence en place ont donc été activé jusqu'au 10 juin 2020, date à laquelle il fut validé que le système de surveillance au sol était réparé. Ce rapport résume la mise en place du projet et la surveillance effectuées lors de cette activation EGS.

1. INTRODUCTION

The Alberta Geological Survey (AGS), a branch of the Alberta Energy Regulator (AER), is responsible for the long-term monitoring of Turtle Mountain (Figure 1). The AGS provides a near real-time remote monitoring network as part of their Turtle Mountain Monitoring Program (TMMP) (Wood and Chao 2019). On April 8, 2020, the AER contacted the Canada Centre for Mapping and Earth Observation (CCMEO) with a request for emergency assistance to monitor Turtle Mountain for deformation using interferometric synthetic aperture radar (InSAR) following the hardware failure of their ground-based InSAR (GB-InSAR) monitoring system. The purpose of the request was to provide a continuation of their monitoring program until the GB-InSAR system could be repaired. This was estimated to take one to two months, but there was additional uncertainty due to the COVID-19 pandemic.

While the GB-InSAR system remained offline, the Turtle Mountain Alert Level was raised to Yellow. This involves monitoring with "increased frequency of data review" to "detect movement trends that are considered non-seasonal" (Wood et al. 2019).

CCMEO agreed to assist and a formal request was sent to Public Safety Canada's regional office in Edmonton via the Government Operations Centre (GOC), who activated Natural Resource Canada's (NRCan) Emergency Geomatics Service (EGS). The EGS provides critical, near real-time geospatial information derived from earth observation satellites to the GOC, the Department of National Defence, and provincial/regional governments during natural disasters. The EGS provides services such as flood extent mapping, river ice monitoring, and infrastructure damage assessment. The EGS was deactivated on June 10, 2020, when the AER confirmed that the GB-InSAR system had been repaired and was collecting valid data. This report summarizes the project setup and monitoring that was performed during the EGS activation.

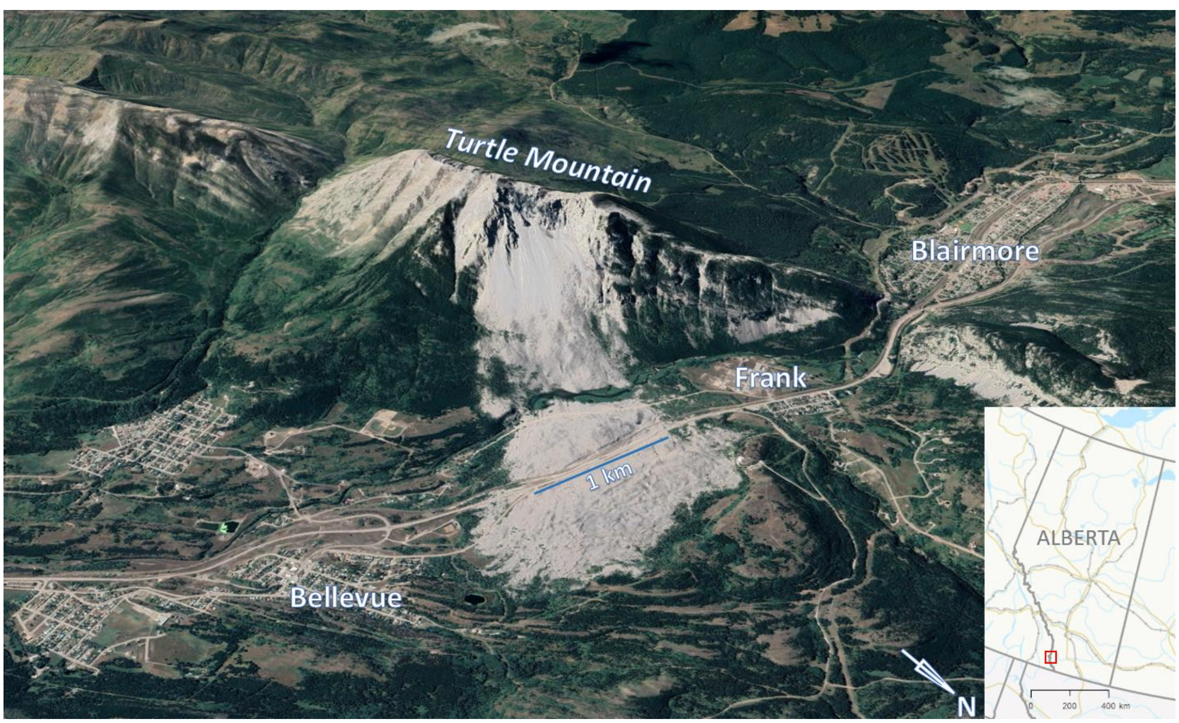

Figure 1: Overview map (Imagery © 2021 CNES/Airbus)

1.1. Historical monitoring and Ground-Based InSAR

The Frank Slide occurred at 4:10 AM on April 29, 1903. In 90 seconds, about 30 million cubic metres of limestone from the east face of Turtle Mountain covered an area of 3 km^2 with an average depth of 14 m of rock debris. The slide killed more than 70 people, and there remains a risk of a second rock avalanche (Read et al. 2005).

Over the next 100 years, many researchers used a wide variety of methods to develop interpretations of the mechanisms of movement and to monitor for early signs of hazardous movements. In 2005, the AGS took ownership of the Turtle Mountain Monitoring System. They are responsible for ongoing monitoring and research focused on understanding the structure and kinematics of movements on the unstable eastern slopes (Yusifbayov et al. 2018).

In 2015, the TMMP began the transition to a near-real-time remote monitoring system. This included lowering the level of response readiness; 24/7 continual on-call status was not warranted by the hazard as observed and evaluated throughout the previous decade of monitoring. GB-InSAR was designated as the primary monitoring sensor, and the non-operational historical monitoring equipment was removed (Wood et al. 2018).

The AGS leases the GB-InSAR monitoring system known as LiSAmobile from Ellegi srl, Milan, Italy. LiSAmobile was installed in June 2014 and had been in nearly continuous operation until April 2020. The AGS receives and reviews monitoring reports on a quarterly basis from Ellegi. Ellegi also provides Quick Reports if an area has displacement values outside of the defined thresholds determined by Ellegi technicians (Wood and Chao 2019).

LiSAmobile consists of a radar head that is mounted on a 2.5 m horizontal track. The sensor travels back and forth along the track every 8.5 minutes, sending microwave pulses and receiving a backscattered signal. The raw data is processed on site and transmitted immediately to Ellegi, who perform quality control and generate measurements of movement along the sensor's line-of-sight (Wood et al. 2018).

Between June 20, 2014 and December 20, 2018, Ellegi observed up to 181 mm of movement toward the sensor along the line-of-sight. The large movements toward the sensor observed in regions D, E, and G (Figure 2) represent rocks falling and accumulating in the debris zones. Movement close to the North Peak (A) was 31 to 181 mm in an area about 4600 m^2. Movement between the North and the South Peak (B) was about 11 mm in an area about 600 m^2. Movement close to the South Peak (C) was about 68 mm in an area about 1200 m^2 The movement detected in the vegetation zone (region F) are considered to be measurement errors due to atmospheric moisture (Wood and Chao 2019).

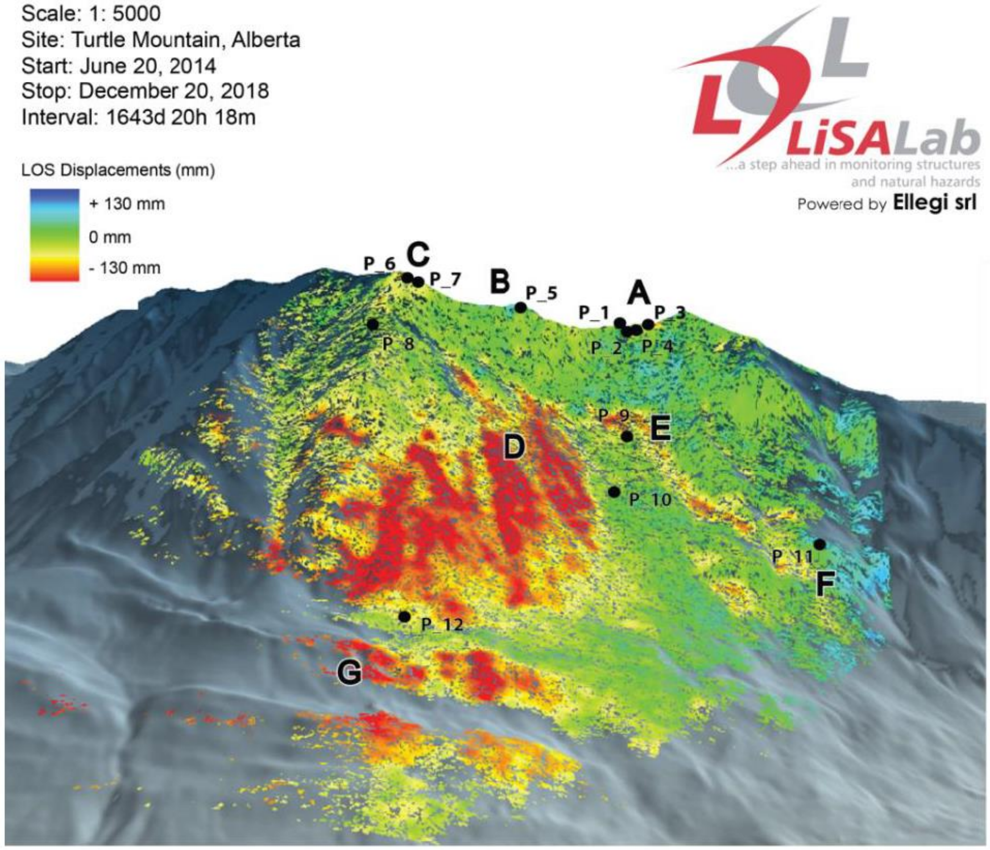

Figure 2: GB-InSAR displacement map from June 20, 2014 to December 20, 2018 (Wood and Chao 2019). GB-InSAR monitoring points (P_1 to P_12) and GB-InSAR monitoring regions (A to G) are reported upon quarterly to the AER.

2. OBJECTIVES

The AER confirmed that their main focus was on the Subsidence, Wedge Sliding, and Toppling zones at the Upper South Peak (Figure 3). The EGS was activated to provide an interim monitoring program at Turtle Mountain while the GB-InSAR system was out of service. The high-level objectives of this monitoring included:

1. Planning and ordering of RADARSAT-2 (RS2) and RADARSAT Constellation Mission (RCM) data that would be suitable for InSAR monitoring
2. Performing historical InSAR analysis on the RADARSAT-2 archive data that can be connected to newly acquired data
3. Performing InSAR analysis on RS2 and RCM data as soon as new data was collected with sufficient coherence
4. Alerting the AGS immediately if any significant movement was observed

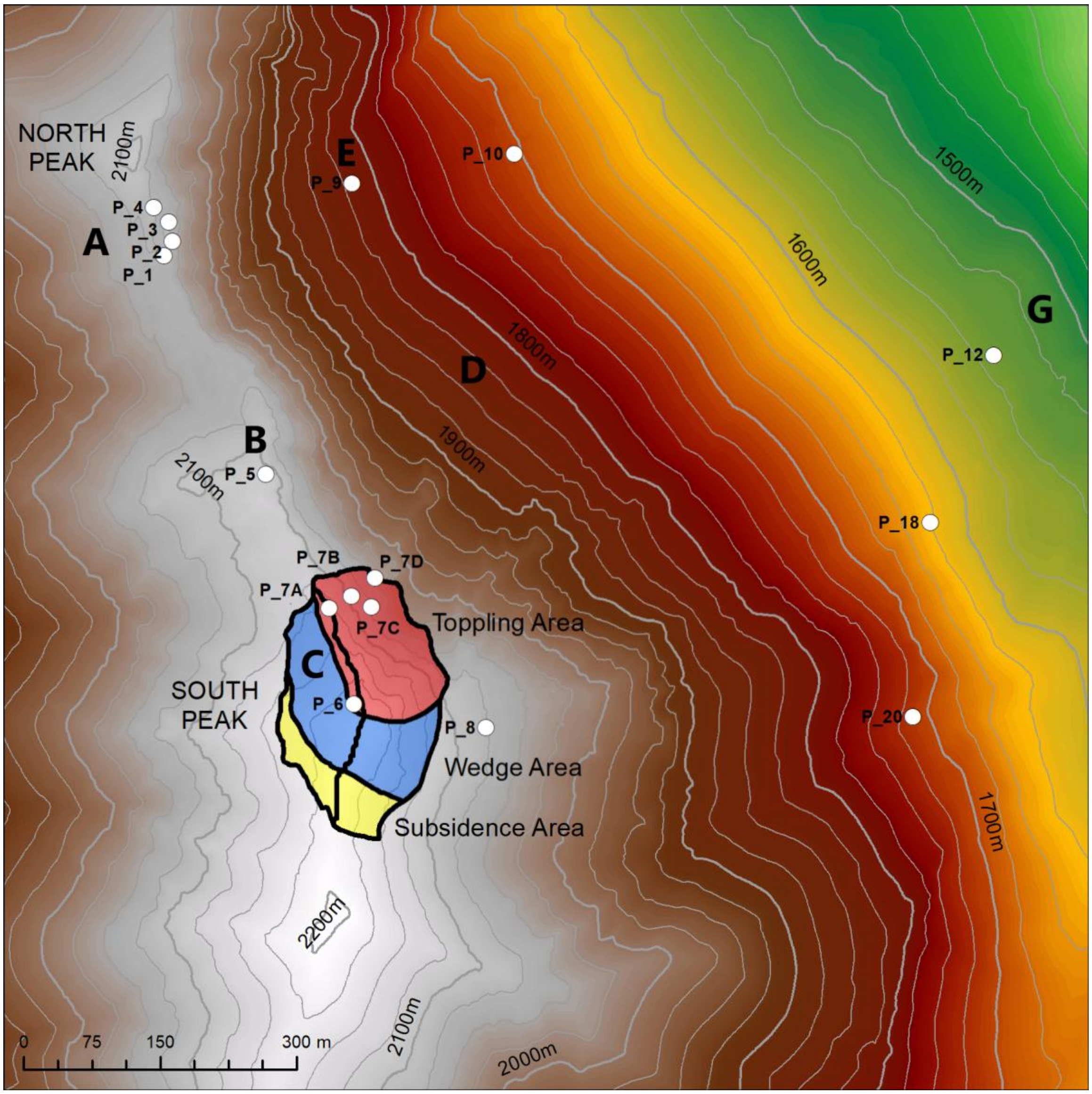

Figure 3: Merged CDSM and LiDAR DEM with deformation zones (red, blue and yellow) and GB-InSAR monitoring points (white).

3. METHODS

Each deformation monitoring program presents a unique challenge, but this methodology can be broadly adapted to similar InSAR monitoring requests in the future.

3.1. Data acquisition

3.1.1. Client data

The AER provided two high-resolution Digital Elevation Models (DEM) derived from LiDAR: a 1 m resolution DEM from 2005 covering about 13 km^2, and a 25 cm resolution DEM from 2016 covering about 1 km^2. These LiDAR DEMs were merged with a 20 m resolution CDSM, all resampled to 3m to match the RCM-3M data. Shapefiles for the displacement zones were derived from Pedrazzini et al. (2012) and were divided into east-facing and west-facing sub-zones using the LiDAR DEM (Figure 3).

The AER also provided a sample report and a Shapefile of the target areas for the GB-InSAR monitoring program, which was helpful for interpreting the InSAR results and providing spatial context for the map products.

Background information was available in the AER Open File Reports as well as the scientific literature. The long history of geological research at Turtle Mountain was crucial for understanding the expected deformation signals, acquiring the right data, and performing the right analysis.

3.1.2. Archived RADARSAT-2 data

A substantial amount of RS2 data exists over Turtle Mountain; over 400 scenes between 2008 and 2020, excluding ScanSAR. However, this data was acquired by a multiple users for a variety of purposes. An InSAR monitoring program requires repeat-pass images which are acquired consistently over a long time period. Most of the InSAR-compatible image stacks were collected for a year or two, excluding winter, and then discontinued. To produce InSAR measurements from 2019 to 2020, the repeat-pass images must at least have been collected consistently in 2019.

The most complete RS2 image stack from 2019 was beam mode Fine Quad 8 Ascending (FQ8A), which consisted of 92 images between 2014 and 2020. This coincides with the GB-InSAR time period, so it should be possible to qualitatively compare the two results where both measurements are coherent (despite differing line-of-sight geometry).

Two other RS2 image stacks were collected in 2019: Fine Wide 1 Descending (F0W1D) and Fine Wide 3 Descending (F0W3D). There were 53 F0W1 images and 53 F0W3 images collected between 2016 and 2019.

The FQ8A, F0W1D, and F0W3D archive images from 2018 and 2019 were processed and analyzed as part of the Preliminary Results delivered on April 29 and May 4, 2020.

Other RS2 image stacks were useful for planning which RCM beam modes to acquire. Eight RS2 image stacks with varying look directions, incident angles, and spatial resolutions were analyzed to assess the impact of their geometry on InSAR coherence, which is a measure of interferogram quality.

The sensor's line-of-sight determines the sensitivity of the InSAR measurements to the movement of the ground. The movement on the ground is projected to the satellite's line-of-sight. If the movement direction is the same as the line-of-sight, the InSAR measurements capture it completely. If the movement direction is orthogonal to the line-of-sight, the signal will be lost completely. The photogrammetric measurements made by Pedrazzini et al. (2012) indicate that the South Peak movements are mostly in the north-east, south-west, and south-east directions. For RS2 and RCM right-looking scenes, the ascending look direction is about 75º (ENE) and descending is about 285º (WNW). The typical range of incident angles are all sensitive to downward motion. Combining both ascending and descending image stacks is ideal for Turtle Mountain. This would maximize coverage of the coherent areas and allow for 2-dimensional decomposition (vertical and east-west) of the measurements where both look directions are coherent.

The incident angle and look direction also determine the degree of shadow and layover/foreshortening. Shadow results in regions with no information returned to the sensor; layover/foreshortening results in information that is "smeared" along the range direction which cannot be attributed to a particular location. For example, an ascending scene with a steep incident angle (e.g. 30º from vertical) will show more layover on the west-facing slope, and less shadow on the east-facing slope. A shallow ascending scene (e.g. 50º) will show less layover on the west-facing slope, and more shadow on the east-facing slope. Descending scenes behave in the opposite manner. As illustrated in Figure 4, the eastern face of Turtle Mountain is steeper than the western face. That means shallow ascending scenes will suffer greatly from shadow on the east face, and steep descending scenes will suffer greatly from layover on the east face. The ideal combination of two beam modes for the east face is a steep ascending stack combined with a shallow descending stack. However, compromises must often be made based on the data available.

The impact of seasonal effects can also be assessed using historical data; the coherence of bare soil and rock in Canada is typically highest in the summer and fall, reduced during the winter, and very low during the spring. Historical analysis can show which regions of the area of interest have sufficient coherence for InSAR analysis throughout the year.

3.1.3. Newly acquired RCM and RADARSAT-2 data

The RCM satellites were launched on June 12, 2019, with a commissioning phase that lasted until early 2020. The 2020 spring flooding and the Turtle Mountain monitoring marked the first operational uses of RCM for the EGS. There were no RCM images acquired over Turtle Mountain before this activation, so all RCM images were newly acquired.

RCM data orders for four different beam modes (3M33A, 3M22A, 3M10A, and 3M7D) began on April 17, 2020. Repeat-pass images were requested every 4 days, but the automated conflict resolution in the order handling system resulted in irregular data acquisition. Between April 17 and June 10, two of the RCM beam mode orders received sufficient data for network analysis: 3M22 (10 images) and 3M7D (7 images). Orders for beam modes 3M33A and 3M10A received only 4 and 3 images, respectively.

Some important parameters for these beam modes are given in Table 1, with the incident angles illustrated in comparison to the mountain slope in Figure 4.

Because of the difficulty in acquiring two of the RCM beam modes, a fourth beam mode (3M42D) was ordered beginning June 5, 2020. Thereafter, 3M42D images were acquired consistently every 4 days. This shows that RCM beam mode selection is important not just for viewing geometry, but also for image acquisition conflict avoidance.

The three primary RS2 archive image stacks (FQ8A, F0W1D, and F0W3D) resumed acquisition on April 23, April 22, and April 19, 2020, respectively.

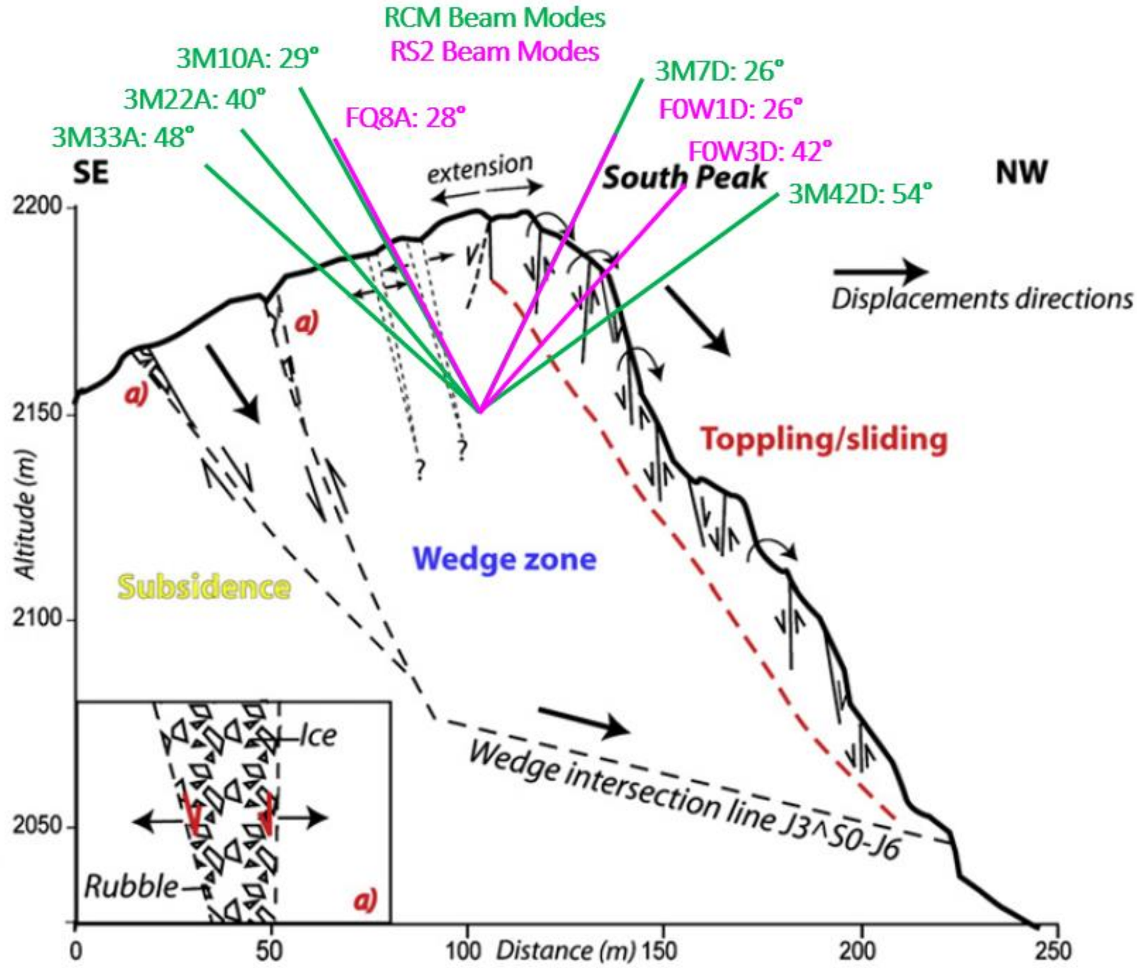

Figure 4: Incident angles of RADARSAT-2 and RCM beam modes acquired in 2020, overlaid on a cross-section of the mountain showing the three deformation zones from Pedrazzini et al. (2012).

Table 1 – SAR beam modes analyzed for this activation

Satellite	Beam Mode	Orbital Direction	Nominal Spatial Resolution	Average Incident Angle	Archived scenes (Pre-Apr 2020)	New Scenes (Apr-Jun 2020)
RS2	FQ8A	Ascending	11 m	28º	88	3
RS2	F0W1D	Descending	10 m	26º	53	3
RS2	F0W3D	Descending	8 m	42º	53	3
RCM	3M33A	Ascending	3 m	48º	0	4
RCM	3M22A	Ascending	3 m	40º	0	10
RCM	3M10A	Ascending	3 m	29º	0	3
RCM	3M7D	Descending	3 m	26º	0	7
RCM	3M42D	Descending	3 m	53º	0	7

3.2. InSAR displacement monitoring

Each new RS2 and RCM scene was processed upon delivery and the interferograms were analyzed visually to detect any fast movement patterns. Variations in atmospheric water content introduce a phase pattern unrelated to ground motion. This pattern is often severe and difficult to model in mountainous areas due to complex weather patterns and large changes in elevation over short distances. However, motion on the order of a centimetre over an extent of several hundred square metres could be observable in a single interferogram. With multiple beam modes, observations of movement can be confirmed or rejected based on complementary measurements.

This processing was performed using the automated InSAR value-added product processor developed by Sergey Samsonov and Jonathan Dudley of the Canada Centre for Remote Sensing. This processor is built using the GAMMA software and will be a component of the Earth Observation Data Management System (EODMS). The EODMS is a geospatial platform provided by Natural Resources Canada open to the general public to discover and download authoritative Canadian Earth Observation raster data.

For this workflow, all images in each stack were coregistered and all possible pairs of images were used to create interferograms. Each interferogram was automatically corrected for topography and orbit baseline, filtered, unwrapped, and converted to a line-of-sight displacement map. There is a trade-off between noise suppression and effective spatial resolution when selecting multilooking and adaptive filter window size parameters. This analysis used no multilooking, with a filter window size of 64 pixels (RCM and RS2 F0W) or 32 (RS2 FQ). Filtering artefacts are visible at the edges of coherent areas and must be interpreted with caution. Deformation patterns that are small in extent would not be detected.

3.3. Time-series analysis

As larger stacks of images are collected, more advanced techniques are possible for detecting slower movement.

After a set of image-to-image displacement maps has been generated, they can be integrated into a single time-series using a technique called SBAS (Small baseline subset). For each pixel, a set of linear equations is solved in the least-squares sense by applying a Singular Value Decomposition (Samsonov 2019).

Areas of low coherence are excluded from the SBAS results. Seasonal variations at Turtle Mountain have an effect on the spatial coherence and there is a trade-off between temporal and spatial coverage. The best spatial coverage can be achieved using data from the snow-free images in a single year between May and October. These single-summer networks can be linked together in a time series by using the highest quality summer-to-summer annual pairs.

Another technique for generating movement time-series is Persistent Scatterers (PS-InSAR). Instead of performing spatial filtering, this involves identifying only the highest-quality targets in the area. This technique was tested using the archived RS2 data, but there were not enough RCM scenes to identify persistent scatterers statistically.

4. RESULTS

4.1. Timeline

April 8	-	Request for assistance; GOC activated EGS
April 17	-	First RCM scene acquired over AOI
April 29	-	Preliminary results for 2018-2019 delivered (RS2 FQ8A)
May 4	-	Preliminary results for 2018-2019 delivered (RS2 F0W1D and F0W3D)
June 10	-	2020 results presented (RCM 3M33A, 3M22A, 3M10A, 3M7D)
	-	AER informed CCRS that GB-InSAR was back online and data had been validated
	-	GOC officially requested EGS to stand down

4.2. Observations

RCM interferograms formed over 4, 8, and 12 day image pairs had very low coherence in April due to snowmelt (Figure 5). Coherence improved throughout May, starting from the lower slope and proceeding to the upper mountain (Figures 6, 7, 8, and 10). By June, the snow had disappeared and coherence was high where there was no vegetation, shadow, or layover (Figures 9, 11, and 12).

Coherence was strongly affected by the incident angle of each beam mode. For example, Figures 5 and 6 show 4-day RCM 3M22A and 3M33A interferograms between May 24-25 and May 28-29. The layover on the western slope is more extreme in the steeper 3M22A; the shadow is longer in the shallower 3M33A. RCM 3M7D and RS2 WF01D (both 26 degrees descending) did not have a suitable viewing geometry for the south peak deformation area. (Figures 8 and 11).

If significant deformation occurred quickly, a fringed or discontinuous phase pattern should be visible in the interferograms from multiple RCM and RS2 beam modes. No significant deformation was observed near the mountain peak in any of the interferograms in May and June 2020 (Figures 6 to 12).

If significant deformation occurred between summer 2019 and summer 2020, a phase pattern should be visible in multiple RS2 year-to-year interferograms (annual pairs). No significant deformation was observed near the mountain peak in annual pairs from RS2 FQ8, F0W1, or F0W3 (Figures 13 to 15).

It should be noted that if too much deformation occurs between scenes, or if the deformation is very heterogeneous, the deformation area may lose all coherence. This type of deformation may be observed using a higher-resolution beam mode or collecting data more frequently.

Each of the following figures illustrates the same area of interest as shown in Figure 2; the white dots and black/green outlines represent the GB-InSAR measurement points and deformation zones described previously. Intensity (dB) represents the amount of radar energy returned to the satellite, scaled from -30 dB (black) to 10 dB (white). Each filtered interferogram represents the change in relative phase between two images, scaled from –π to π (magenta, blue, cyan, green, yellow, red, magenta). Green indicates no relative change; each "fringe" from green to green represents 2.8 cm of change in the line-of-sight distance to the sensor. Coherence, in this case, refers to the magnitude of the complex correlation coefficient between two SAR images. It is normalized between 0 and 1 over a small window, with 0 indicating random phase noise and 1 indicating high quality of phase between the two images.

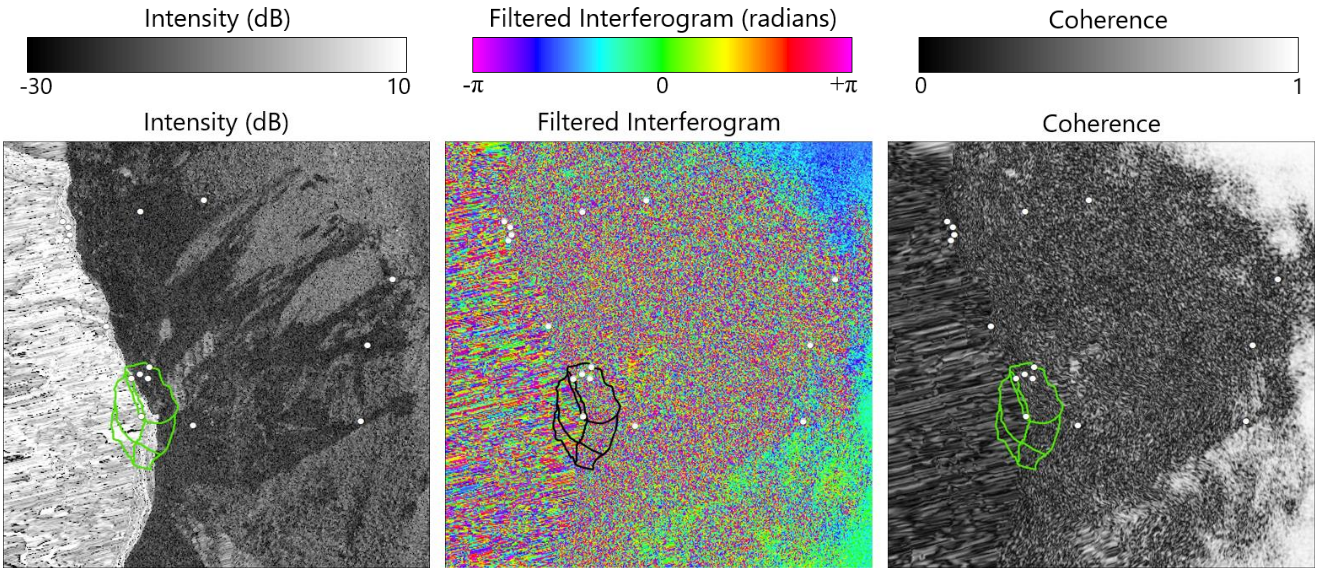

Figure 5: Intensity, interferogram, and coherence for RCM 3M10A, April 21 to April 29, 2020. Similar to other beam modes in April, the snow is in the process of melting; dark patterns from SAR shadow as well as wet soil can be seen in the intensity image, and low coherence is observed over the entire mountain. The layover on the western slope is extreme due to the steep descending incident angle (29º). Unfortunately, no RCM 3M10A data was acquired after April 29.

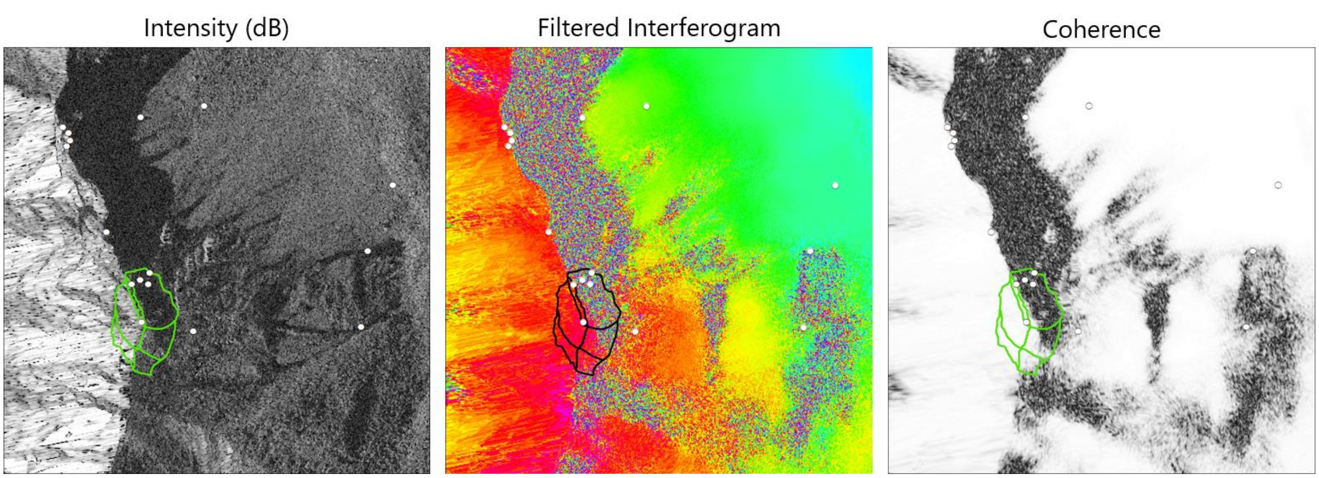

Figure 6: Intensity, interferogram, and coherence for RCM 3M22A, May 24 to May 28, 2020. The snow is mostly melted; high coherence is observed over the western deformation area. There is some layover on the western slope, and some shadows obscure the eastern slope due to the moderate incident angle (40º). A static atmosphere effect can be seen in the interferogram as a transition from green to blue to red as elevation increases.

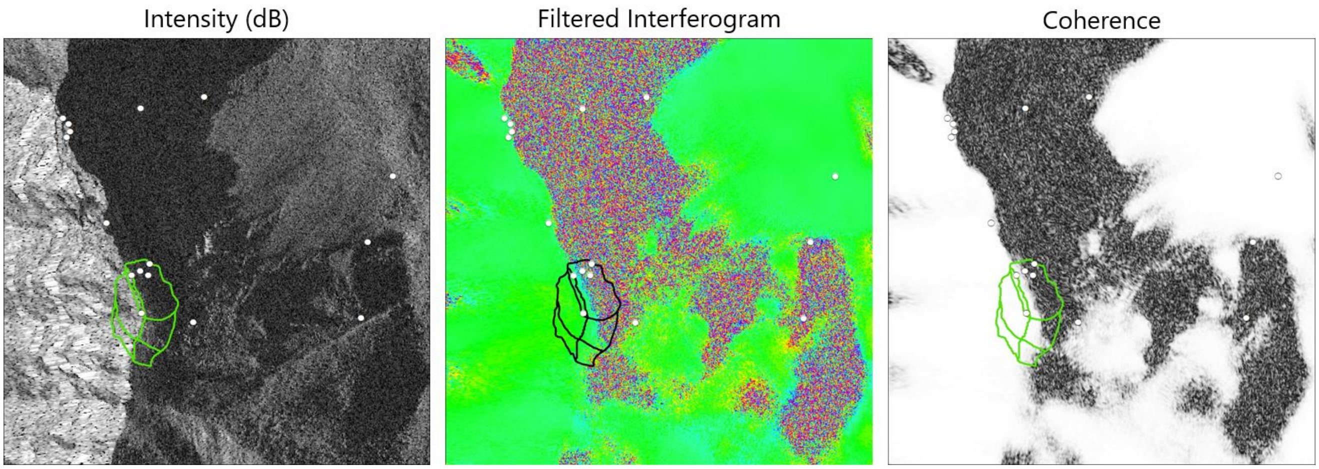

Figure 7: Intensity, interferogram, and coherence for RCM 3M33A, May 25 to May 29, 2020. The snow is mostly melted; high coherence is observed over the western deformation area. There is little layover on the western slope, but long shadows obscure the eastern slope due to the shallow incident angle (48º).

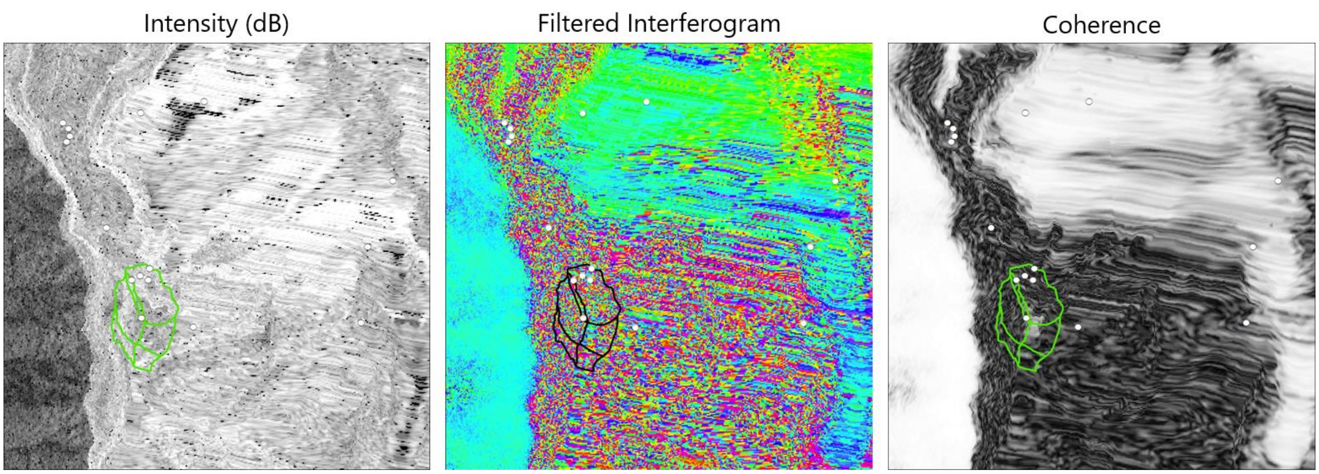

Figure 8: Intensity, interferogram, and coherence for RCM 3M7D, May 27 to June 8, 2020. This is one of the highest coherence interferograms in the 7 image stack, but coherence is still low over the deformation area. The layover on the eastern slope is extreme due to the steep descending incident angle (26º).

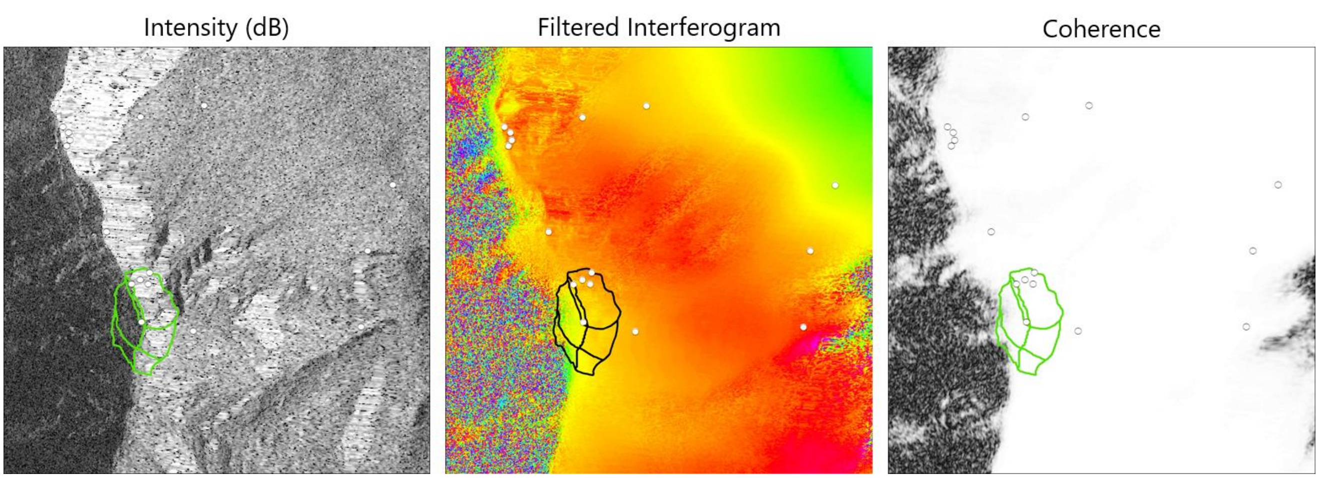

Figure 9: Intensity, interferogram, and coherence for RCM 3M42D, June 6 to June 9, 2020. The snow is fully melted; high coherence is observed over the entire deformation area. There is little layover on the eastern peak, but long shadows obscure the western slope due to the shallow descending incident angle (54º). A combination of static and dynamic atmospheric patterns is visible in the interferogram.

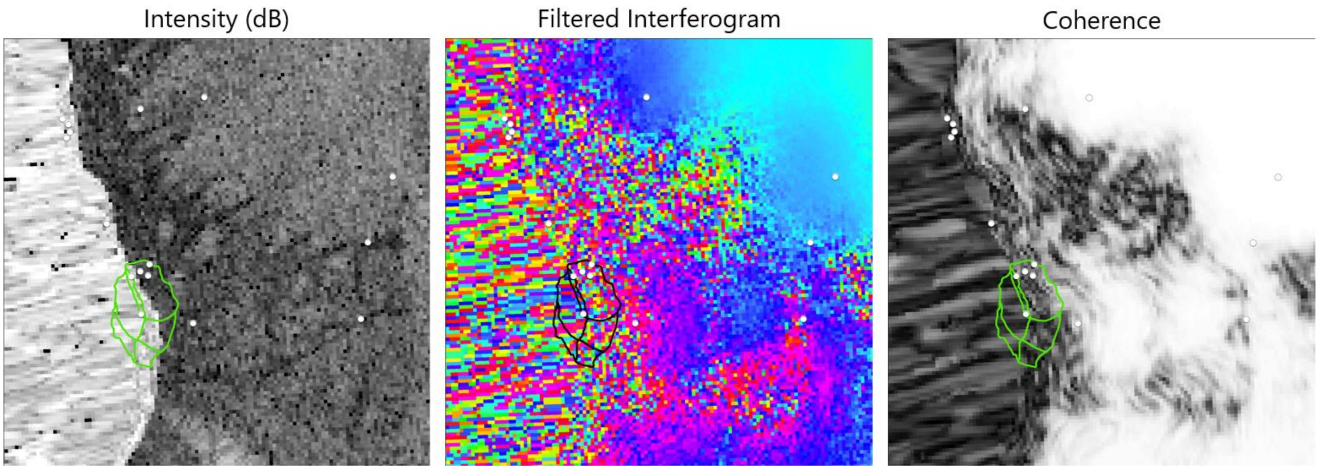

Figure 10: Intensity, interferogram, and coherence for RS2 FQ8A, May 17 to June 10, 2020. The snow is mostly melted, but coherence is low over most of the deformation area. The layover on the eastern slope is extreme due to the steep descending incident angle (26º).

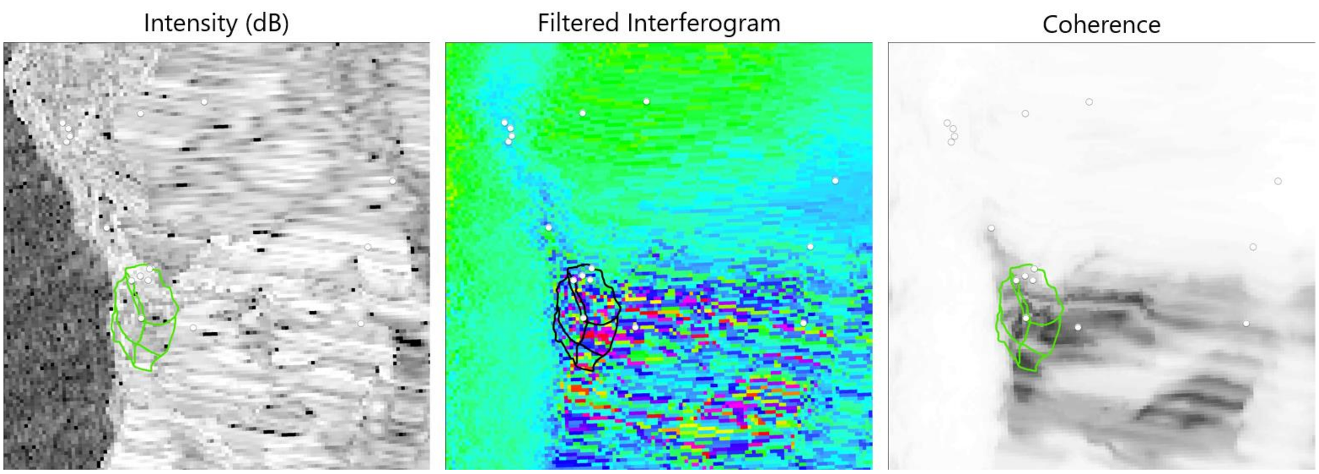

Figure 11: Intensity, interferogram, and coherence for RS2 WF01D, June 9 to July 3, 2020. The snow is fully melted, but coherence is still low over the deformation area. The layover on the eastern slope is extreme due to the steep descending incident angle (26º).

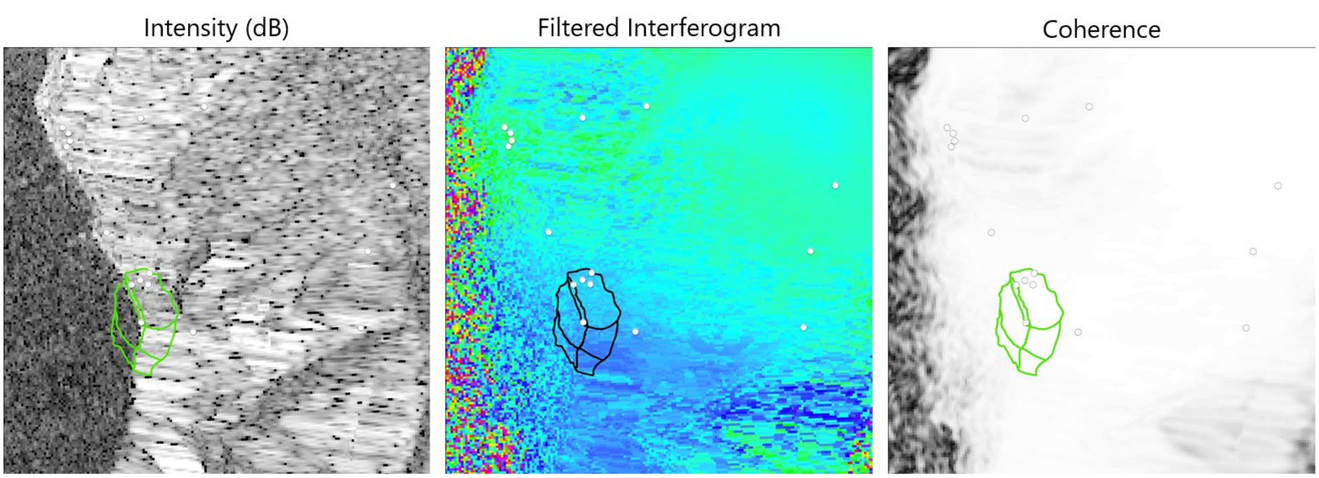

Figure 12: Intensity, interferogram, and coherence for RS2 F0W3D, June 6 to June 30, 2020. The snow is fully melted; high coherence is observed over the entire deformation area. There is little layover on the eastern peak, and some shadows obscure the western slope due to the moderate descending incident angle (42º).

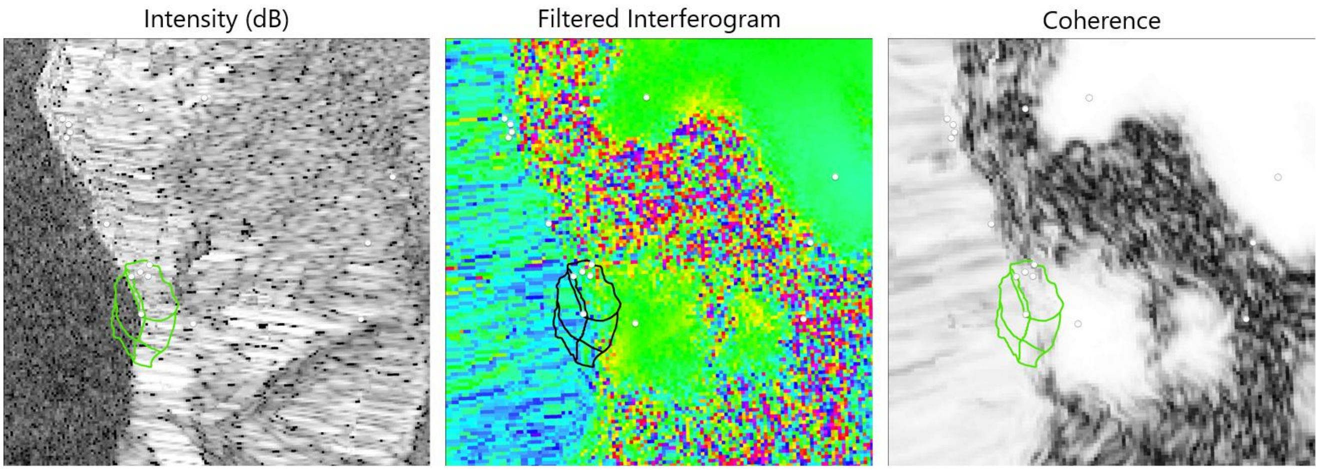

Figure 13: Intensity, interferogram, and coherence for RS2 FQ8A, September 20, 2019 to June 10, 2020. This annual pair shows no significant deformation in the deformation area. However, the area of low coherence could have experienced deformation too strong or heterogeneous to be observed with this image pair.

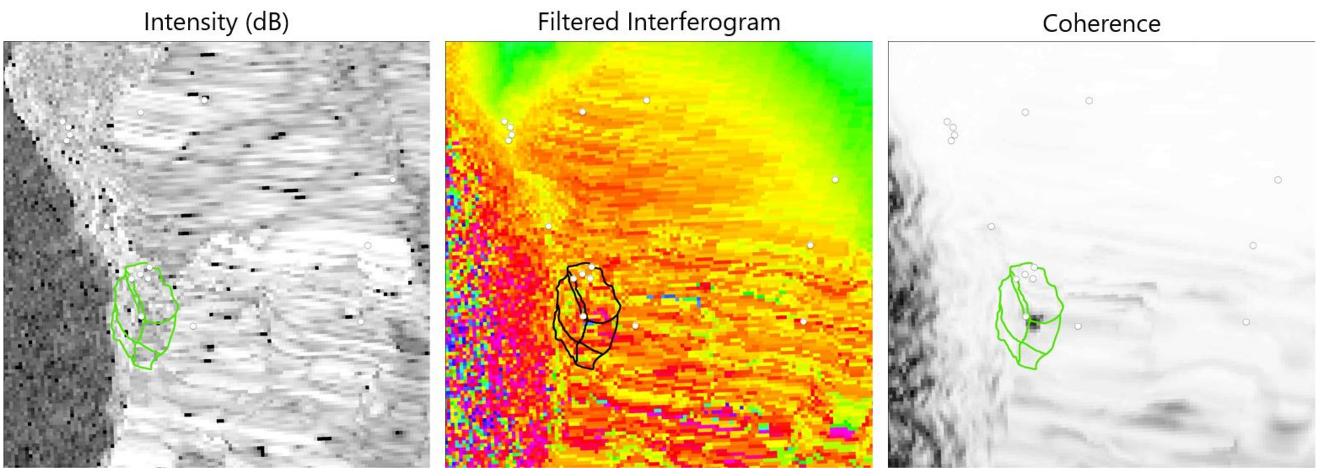

Figure 14: Intensity, interferogram, and coherence for RS2 WF01D, July 9, 2019 to June 9, 2020. This annual pair shows a large dynamic atmospheric phase pattern, but no significant deformation in the deformation area.

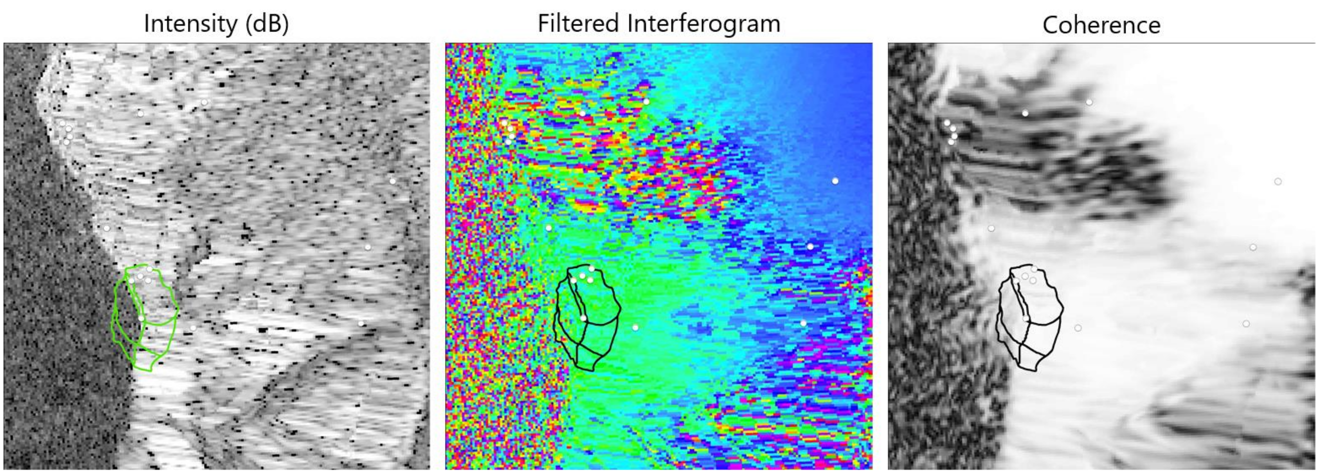

Figure 15: Intensity, interferogram, and coherence for RS2 F0W3D, July 6, 2019 to June 30, 2020. This annual pair shows no significant deformation in the deformation area. However, the area of low coherence could have experienced deformation too strong or heterogeneous to be observed with this image pair.

At Turtle Mountain, short-term SBAS time series are dominated by static and dynamic atmospheric phase patterns (Hosseini et al. 2018); small deformation rates require longer time series to make significant measurements. This atmospheric phase noise can be minimized by choosing annual pair interferograms formed on dates that had similar atmospheric conditions, resulting in a relatively stable phase pattern across the area of interest. It was possible to form such a network of 43 interferograms using the RS2 FQ8A mode; the cumulative deformation from May 25, 2014 to June 10, 2020 is shown in Figure 16. The F0W1D and F0W3D modes did not contain sufficient stable annual pairs to form this type of network. This dynamic atmospheric phase could be removed with spatial filtering and interpolation, but without tight boundaries for the known deformation area, this runs the risk of removing real deformation signals.

For the RS2 FQ8A stack, deformation rates of up to 5 mm/year (LOS) were observed on the east-facing upper and lower slopes between 2014 and 2020. However, a large region of low coherence appears in summer-to-summer annual pairs, suggesting the possibility of widespread non-linear and/or heterogeneous deformation in the lower eastern slope during the winter and spring. Most of the GB-InSAR monitoring points are not coherent in the FQ8A analysis.

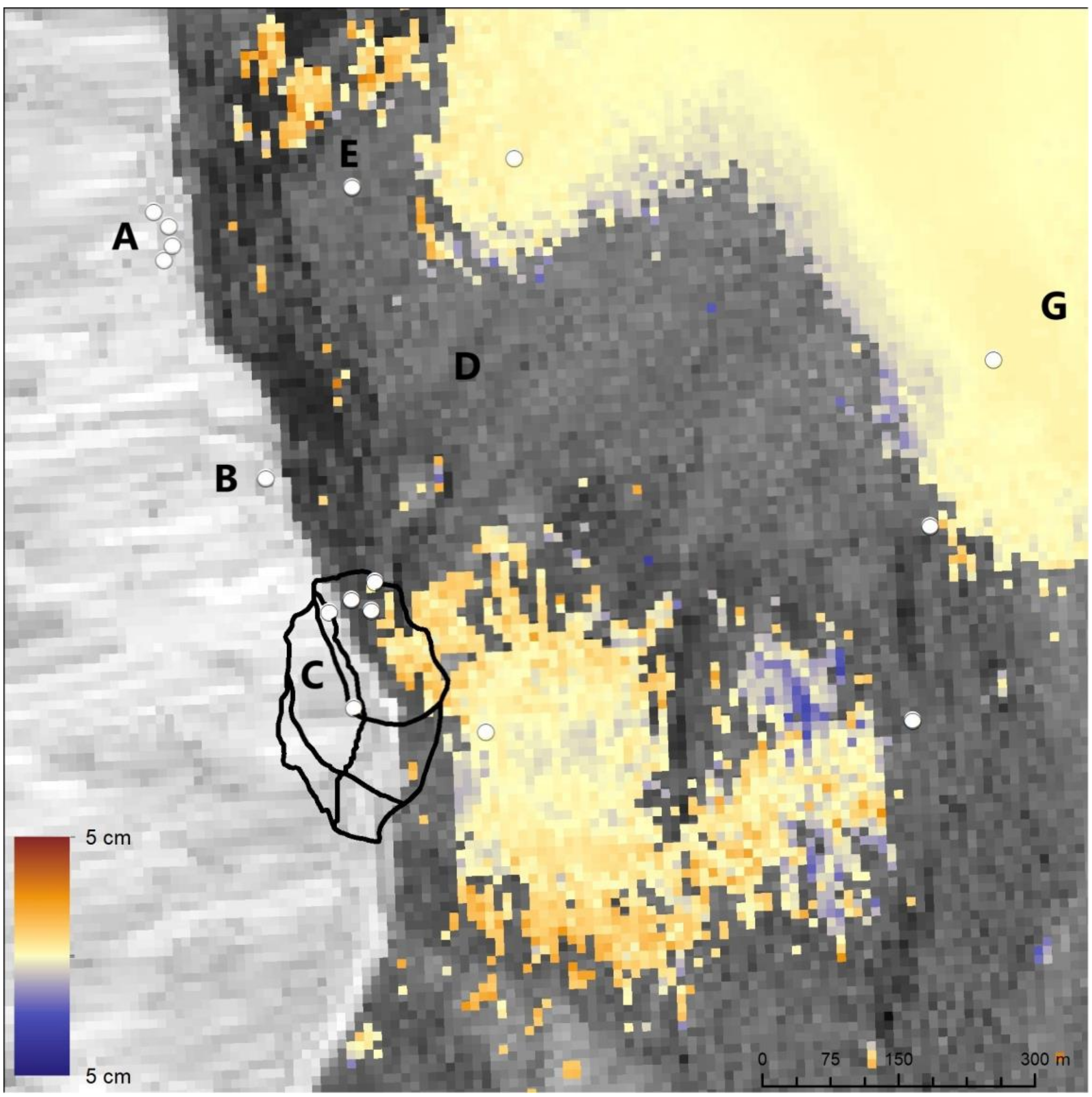

Figure 16: Cumulative line-of-sight deformation for RS2 FQ8A from May 25, 2014 to June 10, 2020.

5. CONCLUSIONS

Between April 8 and June 30, 2020, 40 images were collected by RS2 and RCM satellites over Turtle Mountain. These images were processed quickly after acquisition and no significant deformation was observed in the new data from 2020 and archived data from 2019. Deformation of up to 5 cm in the line-of-sight for RS2 FQ8A was observed between 2014 and 2020.

Setting up an InSAR deformation monitoring project is a complicated process. Each site has unique characteristics that affect the data requirements and processing techniques. It is important for InSAR analysts to understand the geological processes causing past deformation signals and what signals to expect in the future. It also requires an understanding of the causes of decorrelation which affect the spatial and temporal distribution of coherence, which limit when valid measurements are possible. Within a larger deformation monitoring program, similarities between areas of interest can be exploited to produce InSAR deformation measurements more consistently and efficiently.

A well-planned data collection and monitoring strategy is critical for geohazard sites. Emergency deformation monitoring is more effective with good archive data. The RCM order handling system automatically balances the requirements of many users; conflicts can prevent the regular acquisition of repeat-pass InSAR data. Beam mode selection should take into account the likelihood of consistent data acquisition based on past attempts and future modeling.

Coherence is highly variable according to changes in geometry, land cover, seasonality, and time. Data acquisition should be planned to maximize coherence over the AOI by choosing the optimal beam mode and acquisition periods based on ancilliary data: archived SAR data, DEM-derived simulated SAR data, climate data, and land cover data.

For mountainous areas of interest, atmospheric phase is highly variable. Methods exist for removing the atmospheric phase, but it is easy to inadvertently remove the deformation signal as well. The safest way to identify a slow, subtle deformation signal is to identify image pairs with a long temporal baseline where atmospheric conditions were similar for both scenes. If such scenes exist in sufficient quantity, this method maximizes the signal-to-noise-ratio with minimal risk of signal removal.

Ground-based InSAR appears to be well-suited for monitoring the eastern face of Turtle Mountain. In the future, satellite-based SAR may be useful for supplementary deformation monitoring for areas not visible to GBInSAR and identifying motion along other lines-of-sight.

6. ACKNOWLEDGEMENTS

The authors wish to thank Todd Shipman, Subir Chowdhury, and Danielle Wood from the AER/AGS for their ongoing dedication in monitoring Turtle Mountain and their collaboration with NRCan/CCMEO for this emergency activation.

The Canadian Space Agency provided assistance with quickly ordering RS2 and RCM data. Funding was provided by CSA for the InSAR processor under the RCM Data Utilization and Application Plan.

7. REFERENCES

Froese, Corey R., Francisco Moreno, Michel Jaboyedoff, and David M. Cruden. “25 years of movement monitoring on South Peak, Turtle Mountain: understanding the hazard.” *Canadian Geotechnical Journal* 46, no. 3 (2009): 256-269.

Pedrazzini, A., C. R. Froese, M. Jaboyedoff, O. Hungr, and F. Humair. “Combining digital elevation model analysis and run-out modeling to characterize hazard posed by a potentially unstable rock slope at Turtle Mountain, Alberta, Canada.” *Engineering Geology* 128 (2012): 76-94.

Hosseini, F., M. Pichierri, J. Eppler, and B. Rabus. “Staring Spotlight TerraSAR-X SAR Interferometry for Identification and Monitoring of Small-Scale Landslide Deformation.” *Remote Sensing, 10(6)*, 844 (2018).

Read, R. S., W. Langenberg, D. Cruden, M. Field, R. Stewart, H. Bland, Z. Chen et al. “Frank Slide a century later: the Turtle Mountain monitoring project.” *Hungr O, Fell R, Couture RR, Eberhardt (Eds.), Landslide Risk Management. Balkema, Rotterdam*, 713-723 (2005).

Samsonov, S.V. “User manual, source code, and test set for MSBASv3 (Multidimensional Small Baseline Subset version 3) for one- and two-dimensional deformation analysis” *Geomatics Canada, Open File 45*, 1 .zip file (2019).

Wood, D.E. and D. K. Chao. “Turtle Mountain Field Laboratory, Alberta (NTS 82G): 2018 Data and Activity Summary.” *Alberta Energy Regulator, AER/AGS Open File Report 2019-07,* 15 p. (2019).

Wood, D.E., D. K. Chao, J. F. Guo, and T. C. Shipman. “AER/AGS Roles and Responsibilities Manual for the Turtle Mountain Monitoring Program, Alberta” *Alberta Energy Regulator, AER/AGS Open File Report 2019-07*, 15 p. (2019).

Wood, D.E., J. A. Yusifbayov, D. K. Chao, and T. C. Shipman. “Turtle Mountain Field Laboratory, Alberta (NTS 82G): 2016 Data and Activity Summary.” *Alberta Energy Regulator, AER/AGS Open File Report 2018-07*, 24 p. (2018).

Yusifbayov, J. A., D. E. Wood, D. K. Chao, and J. E. Warren. “Turtle Mountain Decommission Project, Alberta (NTS 82G): Summary Report and Historical Signs.” *Alberta Energy Regulator, AER/AGS Open File Report 2018-02*, 13 p. (2018).